MAGNETIC RESONANCE

Jing Ren
Yi Huan
He Wang
YaLi Ge
YingJuan Chang
Hong Yin
LiJun Sun

Seminal vesicle invasion in prostate cancer: prediction with combined T2-weighted and diffusion-weighted MR imaging

H. Wang
Department of Urology,
Xijing Hospital,
Fourth Military Medical University,
Chang Le Western Road No. 15,
Xi'an, 710032,
People's Republic of China

J. Ren · Y. Huan (✉) · Y. Ge ·
Y. Chang · H. Yin · L. Sun
Department of Radiology,
Xijing Hospital,
Fourth Military Medical University,
Chang Le Western Road No. 15,
Xi'an, 710032,
People's Republic of China
e-mail: huanyi3000@163.com
Tel.: +86-29-84775421
Fax: +86-29-84775421

Abstract The aim of this study was to evaluate the usefulness of diffusion-weighted imaging (DWI) in detecting seminal vesicle invasion (SVI). A total of 283 patients underwent conventional MRI and DWI before prostate cancer surgery. The apparent diffusion coefficient (ADC) values of all PCa foci, SVI and seminal vesicle were measured. T2 images alone and then T2 images combined with DWI were scored for the likelihood of SVI. The area under the receiver operating characteristic curve (AUC) was used to assess accuracy. Statistical significance was inferred at $P<0.05$. On pathological analysis, 39 patients had SVI. The ADC values of SVI were significantly lower than those of SV. The AUC for T2-weighted imaging plus DW imaging (0.897) was significantly larger ($P<0.05$) than that for T2-weighted imaging alone (0.779). T2 images combined with DWI shows significantly higher accuracy than T2-weighted imaging alone in the detection of SVI.

Keywords Prostate carcinoma · Seminal vesicle · Magnetic resonance · Diffusion-weighted imaging · Apparent diffusion coefficient

Introduction

In patients with newly diagnosed prostate cancer (PCa), the presence of seminal vesicle invasion (SVI) is associated with high rates of treatment failure and tumor recurrence, and it is an important factor in staging and prognosis that may modify treatment decision and planning [1]. Progression rates reported for these patients range from 40 to 95% [2, 3]. Therefore, accurate detection of SVI is vital to plan the appropriate management of patients with localized prostate cancer. MRI, with high-resolution T2-weighted scans [4], dynamic contrast enhancement [5, 6], and MR spectroscopy [7–9], is increasingly seen as a method that can improve prostate cancer detection, characterization, staging, and treatment.

Diffusion-weighted imaging (DWI) is an MR-based technique that is sensitive to molecular translation of water in biologic tissues due to the random thermal motion of molecules [10]. Several studies have suggested that apparent diffusion coefficient (ADC) values calculated from DWI data may have clinical utility in PCa diagnosis. In recent studies of patients with biopsy-proved PCa, mean ADC values for malignant peripheral zone (PZ) [11] and transition zone [12] tissue were lower than those for nonmalignant PZ and transition zone tissue, despite sizable overlap. The addition of DWI to conventional T2-weighted MR imaging (T2WI) has been found to improve the detection of PCa [13–15].

MR imaging is useful in demonstrating SVI in patients with prostate cancer [3, 16, 17]. In 2008, Kim et al. [18]

reported that T2WI with DWI showed a better diagnostic performance than T2WI alone for predicting SVI. However, in their study a quantitative analysis for SVI was not performed on ADC maps. The purpose of our study was to retrospectively determine the DWI characteristics and ADC values of SVI, and to compare the accuracy of T2-weighted MRI alone and T2 combined with DWI for predicting SVI.

Materials and methods

Patient characteristics

This was a retrospective, single-institution cross-sectional study. Ethical approval for this study was obtained from the local ethics committee. The institutional review board granted exemption status to the study, with a waiver for informed consent.

From January 2007 to November 2008, 283 patients with clinically localized PCa underwent conventional MRI and DWI examinations before radical prostatectomy in our institution. The mean patient age was 68 years (range 56–84 years). None of the patients received neoadjuvant hormonal or radiation therapy before surgery. All patients had a tissue diagnosis of prostate cancer based on biopsy results.

MR technique

MRI was performed on a 3.0-T superconducting unit (Magnetom Trio, Siemens, Erlangen, Germany) using pelvic phased-array coils. In MRI, the prostate was examined from the apex to base. T1-weighted spin-echo (SE) axial images were obtained with the following parameters: TR 550 ms; TE 15 ms; slice thickness 4 mm; interslice gap 0.5 mm; acquisition matrix 320×256; field of view (FOV) 180 mm; number of signals acquired (NSA) 6; acquisition time 4 min. T2-weighted SE axial and coronal images were obtained with the following parameters: TR 4,430 ms; TE 78 ms; slice thickness 3 mm; interslice gap 0.5 mm; acquisition matrix 320×256; FOV 180 mm; NSA 6; acquisition time 5 min. After T1WI and T2WI conventional scans, DWI was acquired through the prostate by utilizing a single-shot spin-echo EPI technique (TR 7,500 ms, TE 80 ms, FOV 400 mm, NEX 9, slice thickness 5 mm, and matrix 128×256) at two b values (0 and 800 s/mm^2). The total acquisition time for DWI was 4 min.

MR imaging analysis

MR imaging analysis was performed separately by two radiologists with 7 and 22 years of experience in prostate imaging at our institution. Each radiologist made a subjective determination regarding the presence of SVI

based on her practical experience and knowledge of previously described SVI MRI features [17, 18]. The main diagnostic criteria used by the radiologists to determine the presence of SVI on MR images were the disruption or loss of the normal architecture of the seminal vesicle, focal or diffuse areas of low signal intensity within the seminal vesicle, low signal intensity within the seminal vesicle causing mass effect, enlarged ejaculatory ducts with low signal intensity, direct extension of the low signal intensity of tumor from the base of the prostate to the seminal vesicle on T2W images [3], and high signal intensity within the seminal vesicle on DWI. T2 images were reviewed first, and then DWI and ADC maps were subsequently reviewed in conjunction with the T2 images. On the basis of the two radiologists' written reports, one author independently and retrospectively scored the likelihood of SVI on a scale of 1–5, with a score of 1 indicating no SVI; 2, probably no SVI (SVI cannot be ruled out, although there is no clear evidence); 3, possible SVI (lesion is suggestive of SVI); 4, probable SVI (lesion is highly suggestive of SVI); and 5, definite SVI [17]. The edge and the contour characteristics of the lesions were defined using the same slices on which regions of interest (ROIs) analyses were performed. The radiologists independently drew ROIs on the ADC maps, and differences in measurement were resolved by consensus. ROIs were also drawn around PC foci, SVI, and SV, respectively. The area of each ROI should be no less than 40 mm^2; the mean $\pm$ standard deviation of ROIs was 81.472 ± 13.928 mm^2. When the ROIs were drawn, great care was taken to exclude both the neurovascular bundle and the urethra to reduce any error in ADC calculations from macroscopic flow. ADCs were calculated for all slices on a voxel-by-voxel basis according to the following equation:

$$\mathrm{ADC}(\mathrm{mm}^2/\mathrm{s}) = \left[1/(b_1 - b_0)\right]\ \ln(S_0/S_1)$$

where S_1 is the signal intensity of a voxel after application of a diffusion gradient and S_0 is the echo magnitude without diffusion gradients applied (b=0 s/mm^2). Diffusion sensitivity is determined by the difference between b_1 and b_0, which in our case was 800 s/mm^2.

Pathological correlation

Step-section pathological maps were available for all patients. The prostatectomy specimens were stained using an India ink tattoo dye and were fixed in 10% formalin for 36 h. The distal 5 mm of the apex was amputated and coned. The remainder of the gland was then serially sectioned from apex to base to obtain transverse slices at 3-mm intervals. Pathological stages were determined for each patient, including the presence or absence of SVI. The

assessment was performed by a urologist with 26 years of experience. These transverse pathological step sections were then matched with the transverse T2-weighted and DW images retrospectively. Great care was taken to minimize the estimated error.

Data analysis

Statistical analyses were performed to assess the statistical differences between the ADC values of PCa foci, SVI, and SV using Student's t test because parameters were normally distributed. Receiver operating characteristic (ROC) curve analyses were performed for all imaging variables to predict SVI. The area under the ROC curve (AUC) was evaluated for models of SVI prediction on the basis of the T2W imaging alone and DW imaging alone. In addition, a model was constructed for the prediction of SVI on the basis of the T2W imaging and DW imaging combined. Comparisons of the AUCs were conducted with the Z test. The sensitivity, specificity, positive predictive value, and negative predictive value for predicting SVI were calculated. $P<0.05$ was considered to indicate a statistically significant difference. The software packages that were used for data analysis were Medcalc and SPSS 11.5.

Results

Histopathological and clinical correlations

On histopathological evaluation, 39 (13.8%) of 283 patients had evidence of SVI and 244 (86.2%) had no SVI after radical prostatectomy. The median Gleason score was 6 (range 3–10), and the mean baseline serum prostate-specific antigen (PSA) level was 12.87 ng/ml (range 4.54–66.97 ng/ml).
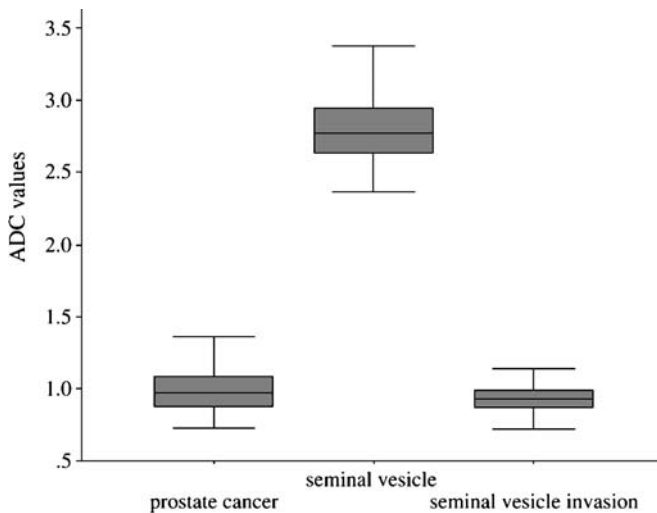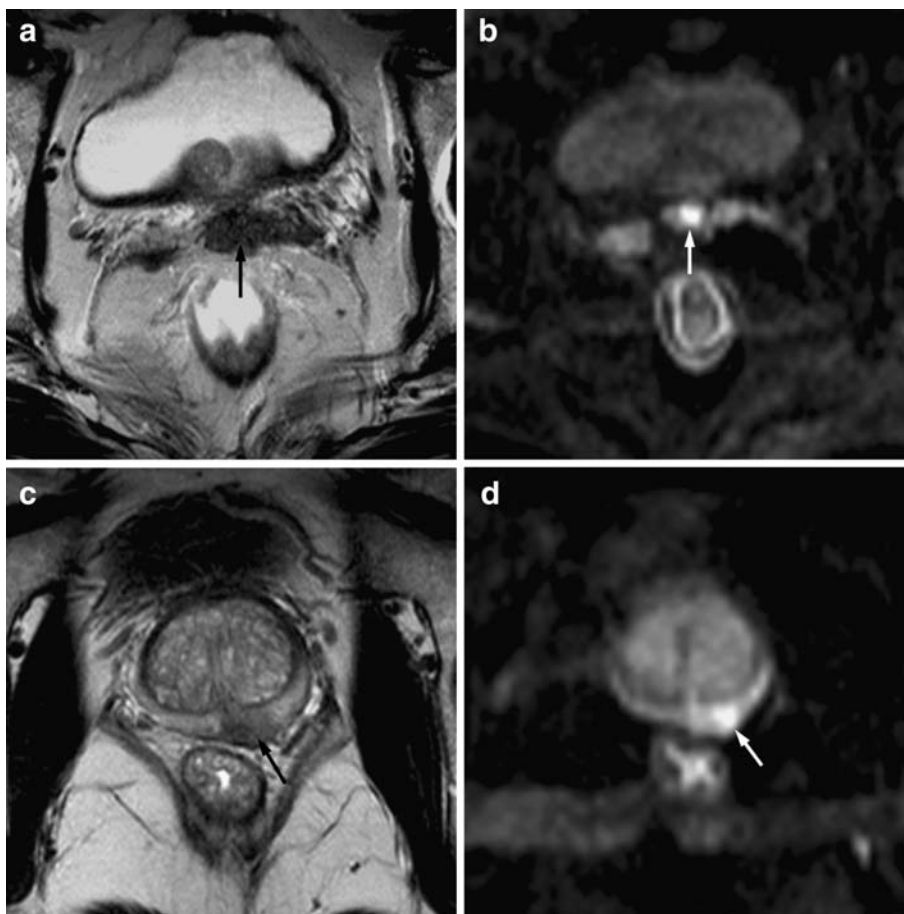
MRI findings and statistical analysis

Among the 39 patients who were pathologically proven SVI, 27 (69.2%, 27/39) cases exhibited low T2 signal intensity mass within SV, 5 (12.8%, 5/39) cases presented low T2 signal intensity due to focal wall thickening of seminal vesicle, and 7 (17.9%, 7/39) cases did not show

Fig. 1 PCa in a 72-year-old man with Gleason score of 7 and PSA level of 12.50 ng/ml. **a** T2-weighted image (TR/TE= 4,430/78 ms), the invaded right seminal vesicle presents low signal intensity mass (*arrows*). **b** DW MR image, SVI presents high signal intensity mass (*arrows*). **c** T2 and DW fusion image (*arrows*). **d** ADC map shows SVI with low signal intensity (*arrows*), where the ADC value of 0.941×10^{-3} mm^2/s is lower than those of left seminal vesicle (2.596×10^{-3} mm^2/s)
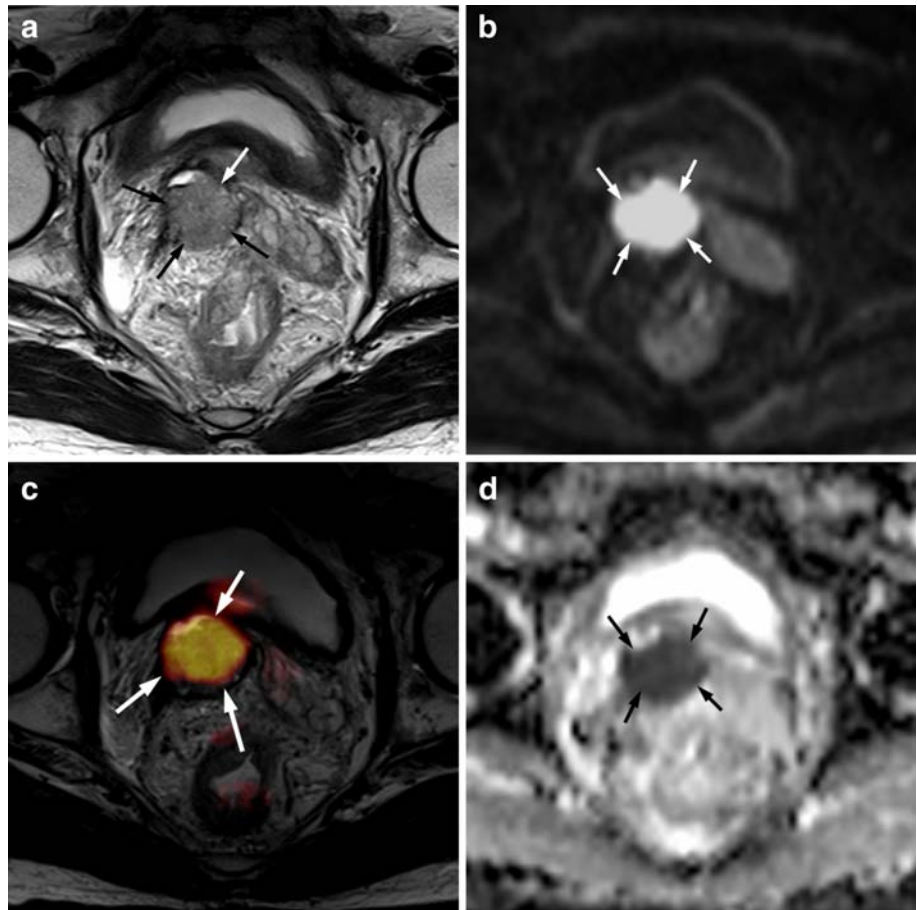
Fig. 2 PCa in a 63-year-old man with Gleason score of 6 and PSA level of 13.78 ng/ml. **a** T2-weighted image (TR/TE= 4,430/78 ms), the invaded seminal vesicles presents low T2 signal intensity mass within SV (*arrow*). **b** DW MR image, SVI presents high signal intensity (*arrow*). **c** T2-weighted image (TR/TE=4,430/78 ms) shows low signal intensity PCa at left peripheral zone of prostate (*arrow*). **d** DW MR image, the PCa shows high signal intensity (*arrow*)

abnormality within SV on T2WI relative to normal SV. While, on DWI, 24 (61.5%, 24/39) cases exhibited high signal intensity, 10 (25.6%, 10/39) cases presented iso-high signal intensity, and 5 (12.8%, 5/39) cases showed

Fig. 3 Boxplot shows comparisons of ADC values among seminal vesicle, SVI, and PCa. The *upper end* of the *vertical lines*, *lower end* of the *vertical lines*, *upper margin* of the *boxes*, *lower margin* of the *boxes*, and *horizontal lines* in the *boxes* represent the upper extremes, lower extremes, upper quartiles, lower quartiles, and medians of the data, respectively
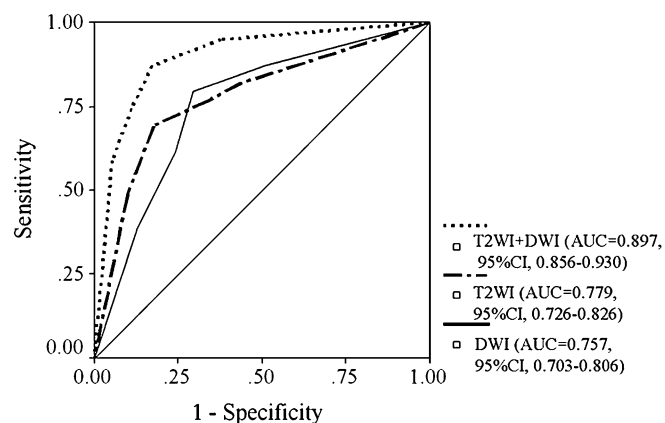
Fig. 4 Receiver operator characteristic (ROC) curves for detection of SVI. The AUC for T2-weighted imaging plus DW imaging (0.897, 95%CI 0.856–0.930) is significantly larger than the AUC for T2-weighted imaging alone (0.779, 95%CI 0.726–0.826) or for DW imaging alone (0.757, 95%CI 0.703–0.806) ($P<0.05$)

Table 1 Sensitivity and specificity for detection of SVI at four cut points of the five-point scoring system

		Cut point 1[a]	Cut point 2[b]	Cut point 3[c]	Cut point 4[d]
T2 weighted	Sensitivity	82.1	76.9	69.2	48.7
	Specificity	56.1	65.6	74.2	90.2
Imaging alone	PPV	23.0	26.3	38.6	44.2
	NPV	95.1	94.7	94.4	91.7
DWI alone	Sensitivity	87.2	79.5	61.5	38.5
	Specificity	49.2	70.5	75.8	87.3
	PPV	22.1	30.1	28.9	32.6
	NPV	96.0	95.0	92.5	89.9
T2 weighted	Sensitivity	94.9	87.2	74.4	59.0
	Specificity	62.3	82.8	88.9	94.7
Imaging + DWI	PPV	28.7	44.7	51.8	63.9
	NPV	98.7	97.6	95.6	93.5

All values are percentages

SVI seminal vesicle invasion, *PPV* positive predictive value, *NPV* negative predictive value

[a] 1=no; 2–5=yes
[b] 1,2=no; 3–5=yes
[c] 1–3=no; 4,5=yes
[d] 1–4=no; 5=yes

iso-low signal intensity within SVI relative to normal SV (Figs. 1, 2).

The mean ADC values of SVI, PCa foci, and SV were $(0.937\pm0.115)\times10^{-3}$ mm^2/s, $(0.993\pm0.158)\times10^{-3}$ mm^2/s, and $(2.803\pm0.234)\times10^{-3}$ mm^2/s, respectively. The ADC values of SVI were significantly lower than those of SV ($t=40.609$, $P=0.000$). There was no significant difference between the ADC values of PCa foci and those of SVI ($t=1.149$, $P=0.258$, Fig. 3).

The AUC for T2-weighted imaging plus DW imaging (0.897, 95%CI 0.856–0.930) was significantly larger than the AUC for T2-weighted imaging alone (0.779, 95%CI 0.726–0.826) or for DW imaging alone (0.757, 95%CI 0.703–0.806) ($Z=5.897$ and 4.550, respectively, $P<0.05$), and there was no significant difference between the AUCs of T2-weighted imaging alone and DW imaging alone ($Z=0.748$, $P=0.454$, Fig. 4). We dichotomized the five-point scoring system and used four cut points to assess the sensitivity, specificity, positive predictive value, and negative predictive value of MRI in the diagnosis of SVI. When cut point 2 was chosen (so that values 1–2 indicated absence of SVI and values 3–5 indicated presence of SVI), sensitivity and specificity were 76.9% and 65.6% for T2-weighted imaging alone and 87.2% and 82.8% for T2-weighted imaging plus DW imaging (Table 1).

Discussion

Patients with local prostate cancer have good prognosis after radical prostatectomy, whereas those with SVI are associated with a worse prognosis [19]. SVI is generally regarded as a marker of poor prognosis at the time of pathological staging

after radical prostatectomy [20]. Invasion may result from direct tumor spread in a contiguous fashion, or tumor infiltration following the course of the ejaculatory ducts or urethra [21]. Therefore, precise pathological tumor staging before treatment is more important than it has ever been. Wang et al. [16, 22] determined that endorectal MR imaging findings had an important role to play in the prediction of SVI. However, conventional MRI could not provide diffusion information about SVI.

In the present study, T2 combined with DWI was able to detect SVI better than T2-weighted imaging alone. The mechanism by which DWI adds diagnostic accuracy to T2 imaging is uncertain. It is possible that the ADC value is more drastically altered by cancer than it is by other factors such as hemorrhage, inflammation, or fibrosis. The ADC values of SVI were significant lower than those of SV; and 34 (87.2%, 34/39) cases of SVI exhibited high signal intensity on DWI. The decrease in ADC values in SVI is attributed to histopathological characteristics of malignant tissue, including enlargement of nuclei, hyperchromatisms, angulation of the nuclear contour, densely packed malignant epithelial cells with little space for mucus or fluid storage, which cause extremely reduced motility of water molecules relative to that of normal tissue, resulting in increased signal on DWI, and decreased ADC values [10, 11, 23–25]. Moreover, SVI is derived from the infiltration of PCa. Therefore, they are histologically associated, and no significant difference between the ADC values of PCa foci and SVI can be detected. On the contrary, seminal vesicles are paired secretory glands that produce seminal fluid [26]. The latter consists of fructose, prostaglandins, protein, and water (the main component) which usually shows low signal on DWI and high ADC values due to the fast molecular translation of water.

In our study, there were 7 (17.9%, 7/39) cases that did not show abnormality within SV on T2WI and 5 (12.8%, 5/39) cases that showed iso-low signal intensity within SVI on DWI; however, this result needs further confirmation. Moreover, the PPVs for SVI were poor. A possible reason might be the difficulty in differentiating the hemorrhage or inflammation in the seminal vesicle from the SVI of PCa [18].

The present study has some limitations. First, by using a pelvic phased-array coil, the image quality was not as good as that using an endorectal coil. But the latter sometimes can stimulate the rectum and cause artifacts. Second, hemorrhage in the SV can result in low signal intensity on T2WI, which may mimic tumor invasion. This feature can lead to false-positive findings for predicting SVI of prostate cancer on T2WI. Finally, our study was retrospective and requires validation in a prospective study.

Notwithstanding these limitations, our initial results suggested SVI had lower ADC values compared with SV. T2 plus DWI MRI is significantly better than T2-weighted imaging alone in the detection of SVI.

References

1. Hricak H, Wang L, Wei DC et al (2004) The role of preoperative endorectal magnetic resonance imaging in the decision regarding whether to preserve or resect neurovascular bundles during radical retropubic prostatectomy. Cancer 100:2655–2663
2. Nguyen PL, Whittington R, Koo S et al (2004) Quantifying the impact of seminal vesicle invasion identified using endorectal magnetic resonance imaging on PSA outcome after radiation therapy for patients with clinically localized prostate cancer. Int J Radiat Oncol Biol Phys 59:400–405
3. Sala E, Akin O, Moskowitz CS et al (2006) Endorectal MR imaging in the evaluation of seminal vesicle invasion: diagnostic accuracy and multivariate feature analysis. Radiology 238:929–937
4. Perrotti M, Han KR, Epstein RE et al (1999) Retrospective evaluation of endorectal magnetic resonance imaging to detect tumour foci in men with prior negative prostastic biopsy: a pilot study. J Urol 162:1314–1317
5. Hara N, Okuizumi M, Koike H et al (2005) Dynamic contrast-enhanced magnetic resonance imaging (DCE-MRI) is a useful modality for the precise detection and staging of early prostate cancer. Prostate 62:140–147
6. Ren J, Huan Y, Wang H et al (2008) Dynamic contrast-enhanced MR imaging of benign prostatic hyperplasia and prostatic carcinoma: correlation with angiogenesis. Clin Radiol 62:153–159
7. Dhingsa R, Qayyum A, Coakley FV et al (2004) Prostate cancer localization with endorectal MR imaging and MR spectroscopic imaging: effect of clinical data on reader accuracy. Radiology 230:215–220
8. Fergus VC, Hui ST, Aliya Q et al (2004) Endorectal MR imaging and MR spectroscopic imaging for locally recurrent prostate cancer after external beam radiation therapy: preliminary experience. Radiology 233:441–448
9. Zakian KL, Eberhardt S, Hricak H et al (2003) Transition zone prostate cancer: metabolic characteristics at [1]HMR spectroscopic imaging—initial results. Radiology 229:241–247
10. Choi YJ, Kim JK, Kim N et al (2007) Functional MR imaging of prostate cancer. Radio Graphics 27:63–77
11. Hosseinzadeh K, Schwarz SD (2004) Endorectal diffusion-weighted imaging in prostate cancer to differentiate malignant and benign peripheral zone tissue. J Magn Reson Imaging 20:654–661
12. Sato C, Naganawa S, Nakamura T et al (2005) Differentiation of noncancerous tissue and cancer lesions by apparent diffusion coefficient values in transition and peripheral zones of the prostate. J Magn Reson Imaging 21:258–262
13. Shimofusa R, Fujimoto H, Akamata H et al (2005) Diffusion-weighted imaging of prostate cancer. J Comput Assist Tomogr 29:149–153
14. Haider MA, Kwast TH, Tanguay J et al (2007) Combined T2-weighted and diffusion-weighted MRI for localization of prostate cancer. AJR 189:323–328
15. Tanimoto A, Nakashima J, Kohno H et al (2007) Prostate cancer screening: the clinical value of diffusion-weighted imaging and dynamic MR imaging in combination with T2-weighted imaging. J Magn Reson Imaging 25:146–152
16. Wang L, Hricak H, Kattan MW (2007) Prediction of seminal vesicle invasion in prostate cancer: incremental value of adding endorectal MR imaging to the Kattan nomogram. Radiology 242:182–188
17. Jung DC, Lee HJ, Kim SH (2008) Preoperative MR imaging in the evaluation of seminal vesicle invasion in prostate cancer: pattern analysis of seminal vesicle lesions. J Magn Reson Imaging 28:144–150
18. Kim CK, Choi D, Park BK, Kwon GY, Lim HK (2008) Diffusion-weighted MR imaging for the evaluation of seminal vesicle invasion in prostate cancer: initial results. J Magn Reson Imaging 28:963–969
19. Cornud F, Flam T, Chauveinc L et al (2002) Extraprostatic spread of clinically localized prostate cancer: factors predictive of pT3 tumor and of positive endorectal MR imaging examination results. Radiology 224:203–210
20. Potter SR, Epstein JI, Partin AW (2000) Seminal vesicle invasion by prostate cancer: prognostic significance and therapeutic implications. Rev Urol 2:190–195
21. Secaf E, Nuruddin RN, Hricak H, McClure RD, Demas B (1991) MR imaging of the seminal vesicles. AJR 156:989–994
22. Wang L, Zhang JB, Schwartz LH et al (2007) Incremental value of multiplanar cross-referencing for prostate cancer staging with endorectal MRI. AJR 188:99–104
23. Pickles MD, Hons BS, Gibbs P, Sreenivas M, Turnbull LW (2006) Diffusion-weighted imaging of normal and malignant prostate tissue at 3.0T. J Magn Reson Imaging 23:130–134
24. Miaoa H, Fukatsu H, Ishigaki T (2007) Prostate cancer detection with 3-T MRI: comparison of diffusion-weighted and T2-weighted imaging. Eur J Radiol 61:297–302
25. Matsuki M, Inada Y, Tatsugami F, Tanikake M, Narabayashi I, Katsuoka Y (2007) Diffusion-weighted MR imaging for urinary bladder carcinoma: initial results. Eur Radiol 17:201–204
26. D'Amico AV, Renshaw AA, Sussman B, Chen MH (2005) Pretreatment PSA velocity and risk of death from prostate cancer following external beam radiation therapy. JAMA 294:440–447